Selective Detection and Quantification of Modified DNA with Solid-State Nanopores

By: Autumn T. Carlsen, Osama K. Zahid, Jan A. Ruzicka, Ethan W. Taylor, and Adam R. Hall

Autumn T. Carlsen, Osama K. Zahid, Jan A. Ruzicka, Ethan W. Taylor, and Adam R. Hall. Selective Detection and Quantification of Modified DNA with Solid-State Nanopores. *Nano Letters.* 2014, 14, 10, 5488–5492. https://doi.org/10.1021/nl501340d

Abstract:

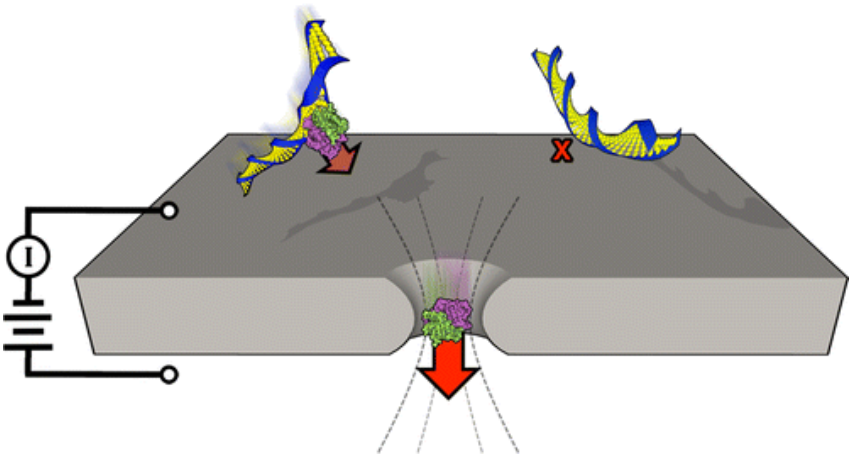

We demonstrate a solid-state nanopore assay for the unambiguous discrimination and quantification of modified DNA. Individual streptavidin proteins are employed as high-affinity tags for DNA containing a single biotin moiety. We establish that the rate of translocation events corresponds directly to relative concentration of protein–DNA complexes and use the selectivity of our approach to quantify modified oligonucleotides from among a background of unmodified DNA in solution.

Keywords: solid-state nanopores | modified DNA | double-strand DNA | monobiotinylated dsDNA

Article:

Immunoprecipitation and pull-down assays are workhorses in biochemistry. With the ability to discriminate specific substrates in heterogeneous mixtures, they play important roles in a wide range of fields, including proteomics,[1-3] epigenomics,[4-7] and transcriptomics.[8, 9] However,

despite their broad utility these well-established strategies have limitations. Besides requiring large sample sizes, they are labor-intensive and are not inherently quantitative, typically requiring subsequent polymerase chain reaction[10] or enrichment[11] for downstream analysis. For these reasons, quantitative technologies with single-molecule sensitivity may offer important advantages.[5]

Hinging on the Coulter principle, solid-state (SS-) nanopores[12, 13] have been employed extensively for molecular resistive-pulse sensing. In these experiments, the temporary presence of a single molecule passing through a narrow pore alters the coincident flow of ions, thereby creating a unique electronic signature in the measured ionic current. Analysis of these signatures (or events) offers insight into molecular structure,[14, 15] surface charge,[16, 17] and pore-molecule interactions.[18, 19] With potential applications ranging from DNA sequencing[20] to biomarker identification,[21] this powerful detection platform has been used to probe a diverse set of materials, including nucleic acids,[22-24] proteins,[25-27] and nonbiological nanoparticles.[28-30]

Recently, several groups have reported progress toward SS-nanopore differentiation of structural[31-33] or chemical[34, 35] variations in nucleic acid molecules. However, such studies often rely on subtle shifts in event characteristics that can introduce uncertainty. In this paper, we present an assay that enables unambiguous identification of double-strand (ds) DNA modified with a single biotin moiety. Using a high-affinity protein tag (monovalent streptavidin, MS) to label modified oligonucleotides, we determine that translocation event rate correlates with protein–DNA complex formation. We speculate on the mechanism underlying this finding and then exploit its specificity to quantify modified DNA directly in solution with unmodified oligonucleotides.

SS-Nanopore Discrimination of Monobiotinylated dsDNA

Figure 1a shows a schematic of the SS-nanopore measurement approach utilized here. An electrical bias is applied across a thin-film membrane with a single nanopore immersed in electrolyte solution (see Methods). This facilitates the electrokinetic translocation of molecules (or molecular complexes) through the pore, each of which can produce an ionic current event. We first use this technique to measure MS (Figure 1b left) and monobiotinylated 90 bp dsDNA (bio90, Figure 1b center) individually at concentrations of 8 and 1 μM, respectively. Over a range of 50–200 mV, few events can be identified for either molecule. However, when MS and bio90 are incubated together at a molar ratio of 8:1 (MS:bio90) prior to measurements, we observe a remarkable increase in the number of events per unit time (Figure 1b right). The event rate of the admixture is consistently more than an order of magnitude greater than that of either constituent molecule alone; at 200 mV applied voltage, for example, the MS/bio90 complex yields a rate of $23.3 \pm 0.9\ s^{-1}$, while the event rates of MS and bio90 individually are 0.09 ± 0.04 and $1.1 \pm 0.2\ s^{-1}$, respectively. In order to verify that the MS/bio90 events correspond to actual translocations rather than stochastic interactions between the complex and the nanopore, we reverse the polarity of the applied voltage during our measurement and observe "recapture events"[36, 37] (see Supporting Information Figure 1). Translocations are further supported by the voltage dependence[38] observed for MS/bio90 event durations (Supporting Information Figure 3).

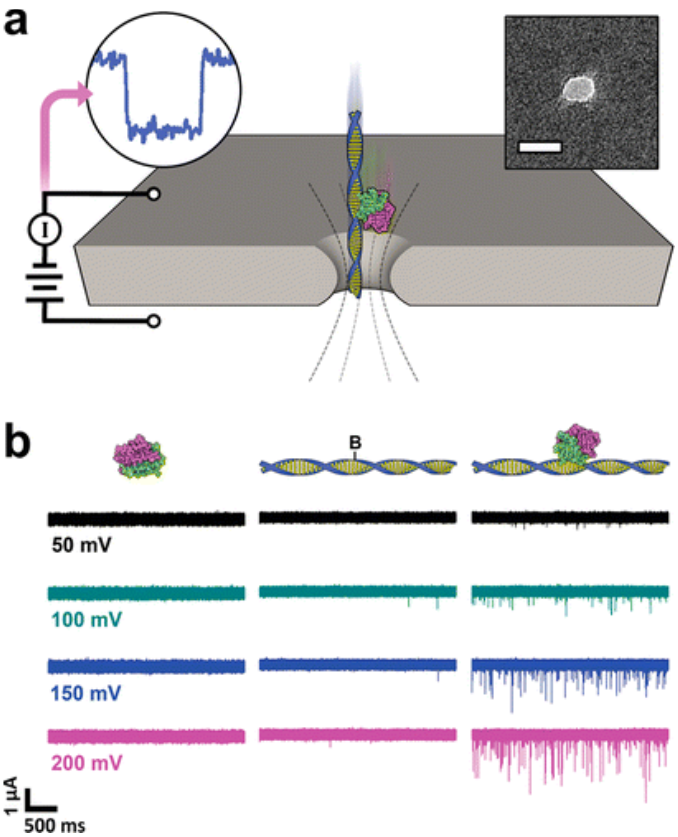

Figure 1. SS-nanopore measurement. (a) Schematic diagram of the experimental system. A bias is applied across a SS-nanopore in a SiN membrane, inducing electrokinetic translocation of protein–DNA complexes in electrolyte solution. Upper left shows the shape of a resistive pulse measured during a translocation event. Right inset: transmission electron micrograph of a typical SS-nanopore formed with conditions identical to those used here. Scale bar is 10 nm. (b) Raw current traces obtained for MS alone (left), bio90 alone (center), and MS incubated with bio90 at a molar ratio (MS:bio90) of 8:1 (right) over a range of voltages. Investigated molecules are shown schematically above each column ("B" represents the biotin moiety). Only the coincubated material produces significant events.

What accounts for the extraordinary differences in the event rates that we observe? Although neither the MS nor bio90 alone yields a significant number of events over the investigated voltage range, we suggest differing explanations for each. For the MS, recent work[26] comparing experimental data to the Smoluchowski theory[39] suggests that the translocation of proteins through SS-nanopores typically occurs too rapidly to be resolved by conventional systems like the one employed here. Indeed, Larkin et al.[27] demonstrated that the enhanced time-resolution of a high-bandwidth system is capable of resolving far more protein translocation events than are detectable by standard electronics. The significant negative charge of our MS (see Methods) will contribute to a strong electrophoretic driving force, potentially reducing translocation time further. We therefore conclude that the absence of observed MS events results from the bandwidth limitations of our apparatus, which allow a significant number of protein molecules to translocate undetected. Conversely, we attribute the small number of events measured for bio90 to infrequent translocations. Storm et al.[40] showed experimentally that dsDNA dwell times scale with molecular length as a power-law with exponent 1.27. Their results were obtained using SS-

nanopores of similar diameter to those employed here and with a comparable voltage. Assuming that the scaling factor holds for small molecular lengths (Wanunu et al.[19] reported similar scaling for short dsDNA), we estimate that 90 bp dsDNA should translocate in ~50 μs; a value that is resolvable by our electronics. Indeed, of the few events that we observe with bio90 alone, most yield a dwell time near this value (see Supporting Information Figure 4). Thus, we conclude that under the low-voltage conditions investigated here, the translocation event rate for bio90 is minimal.

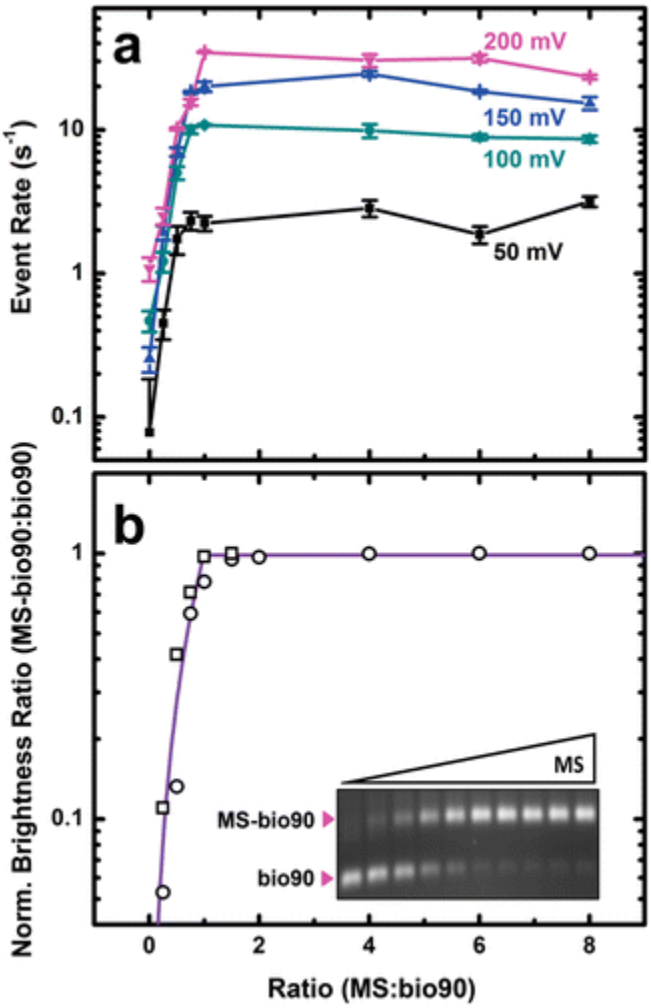

Figure 2. MS/bio90 titration experiments. (a) Semilog plot showing stoichiometric dependence of SS-nanopore translocation event rate over a range of applied voltages. (b) Semilog plot (normalized) showing stoichiometric dependence of band intensity for MS/bio90 complex relative to bio90 measured from EMSA. Circles and squares are data from two separate assays. Inset shows an example gel (circle symbols in plot).

The dichotomy between these two explanations offers a possible mechanism for the increase in event rate observed for the admixture of MS and bio90. When the molecules form a complex, the large net electrical force experienced by MS alone is countered by a significant viscous drag imparted by the bio90. We therefore propose that the combination of these forces results in translocations that are slow in comparison to MS alone and are thereby resolvable with our

apparatus. Importantly, this results in selective isolation of target DNA rather than exclusion determined, for example, by SS-nanopore dimensions.[21]

In order to investigate the system further, we next perform a series of SS-nanopore measurements in which MS is titrated against a constant amount (1 μM) of bio90. Over all investigated voltages, we observe that the measured event rate rises dramatically up to a molar ratio of 1:1 (Figure 2a). However, from unity up to a molar ratio of 8:1 (MS:bio90), additional MS does not increase the event rate further. This is a result of the limited supply of dsDNA needed to form nucleoprotein complexes; the protein has an extremely low off rate[41] ($\sim 10^{-5}$ s^{-1}) and each oligonucleotide contains only a single biotin moiety, so we expect that nearly all bio90 in solution will be bound at or above an equimolar concentration. Comparing our translocation results to an electromobility shift assay (EMSA) performed with MS and bio90 over the same stoichiometric range, we observe a strikingly similar trend (Figure 2b). These data support our assertion that virtually all observed translocation events for the admixture correspond to MS/bio90 complexes. Additional evidence of the high specificity of this approach is provided by control measurements in which nonbiotinylated dsDNA incubated with MS yields a negligible event rate, equivalent to bio90 alone (see Supporting Information Figure 5).

Selective Quantification of Modified Oligonucleotides

In Figure 3, we examine admixture event rates up to a molar ratio of 1:1 and find a linear dependence on applied voltage. This implies that the capture process for the MS/bio90 complex is governed by diffusion rather than by interactions with the pore, which is in agreement with previous studies.[36] Importantly, the observed trend offers a route toward quantification of MS/bio90 complexes in solution. It has been demonstrated elsewhere[19, 26, 32] that event frequency varies with molecular concentration. Because nearly all events observed in our system can be attributed exclusively to the translocation of complexes, the linear fits in Figure 3 link the concentration of MS/bio90 in solution to specific event rates produced at a given voltage. The measurements described thus far have been performed in a protein-limited regime (MS:bio90 < 1:1), and so the measured event rate has facilitated quantification of MS/bio90 complexes in a background of unconjugated bio90. However, the same approach could in principal be used to quantify biotinylated oligonucleotides in a heterogeneous solution with nonbiotinylated DNA as well.

To investigate this possibility, we conduct a blind test on two samples prepared by a third party. Each of these samples contains a different mixture of biotinylated and nonbiotinylated 90 bp dsDNA mixed to a total concentration of 1 μM (equivalent to that of the measurements described above). To ensure that all bio90 is conjugated, both solutions are incubated with MS at a concentration of 4 μM. As described in the previous sections, MS alone produces a negligible number of measurable events, and so excess protein does not perturb the measurements. SS-nanopore analysis reveals a linear relationship between applied voltage and event rate for both samples, as expected (see Supporting Information Figure 6). Comparing the event rates obtained from the two blind samples to our prior measurements (Figure 4), we derive a value for the bio90 concentration in each: 850 ± 35 nM in Sample 1 and 520 ± 20 nM in Sample 2. Remarkably, these experimentally determined concentrations are in excellent agreement with the prepared values of 800 ± 20 and 480 ± 20 nM, respectively. These results demonstrate that our SS-

nanopore approach is uniquely capable of quantifying DNA having single nucleotide biotin modifications selectively, even within a mixed sample.

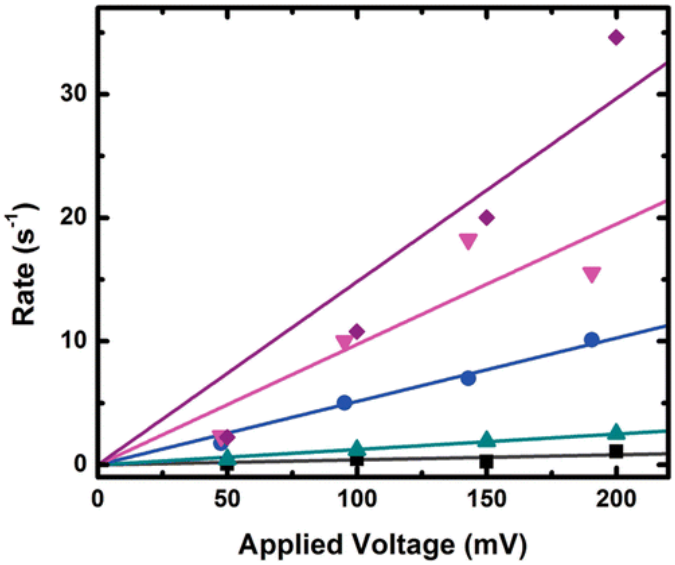

Figure 3. Voltage dependence of event rate. Event rates corresponding to specific MS/bio90 stoichiometries plotted over a range of applied voltages. From bottom to top, molar ratios (MS:bio90) are 0:1 (squares), 1:4 (upward triangles), 1:2 (circles), 3:4 (downward triangles), and 1:1 (diamonds). Solid lines are linear fits to each ratio set (color indicated).

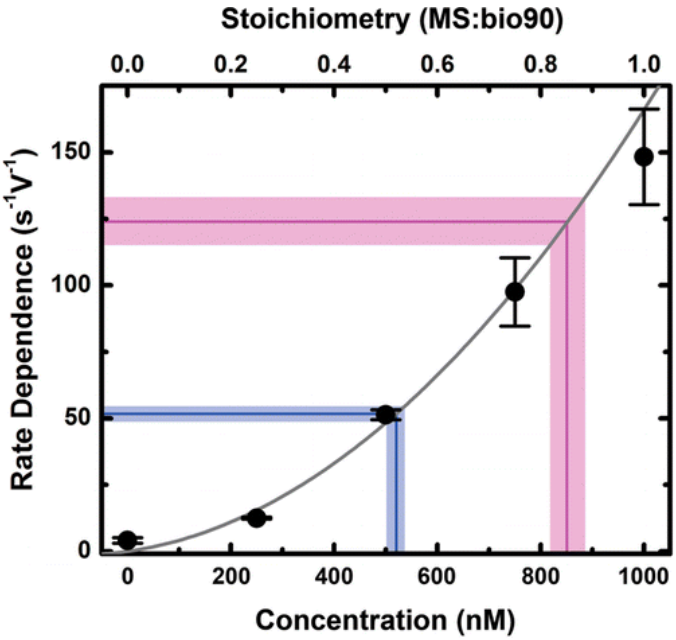

Figure 4. Selective determination of bio90 concentration within a mixture. Solid data points indicate event rate dependence (i.e., slopes from Figure 3) plotted against MS/bio90 concentration. Solid gray line is a second-order polynomial fit to the data. Experimentally derived event rate values for samples prepared in blind experiments are shown as magenta (Sample 1) and blue (Sample 2) lines extending from *y*-axis. Shaded regions represent error.

Discussion

In this study, we have demonstrated highly specific detection and quantification of monobiotinylated dsDNA using SS-nanopores. We performed our detection through selective conjugation with a streptavidin protein containing a single biotin-binding domain. Under the experimental conditions investigated, we observed that the MS/bio90 complex produced a cascade of easily resolved translocation events, which is in stark contrast to either constituent molecule individually. While the DNA constructs used here featured an internal biotin near the center of the molecule (see Methods), additional measurements indicate that the effect is not dependent on the position of the biotin moiety. The variation in translocation behavior was attributed to structure-dependent differences in net driving force, resulting in a dramatic increase in resolvable translocation events for the nucleoprotein complex as compared to DNA or protein alone. By studying stoichiometric effects, we showed that measured event rate correlated to the (partial) concentration of MS/bio90 conjugates in solution. Finally, we exploited the specificity of our measurement and the relationship between event rate and concentration to achieve selective quantification of modified oligonucleotides within a background of unmodified DNA. Upon examination of two different blind samples, we found excellent agreement with prepared values, validating our approach as a quantitative detection technique. An analogue to conventional approaches like immunoprecipitation, our technique offers unique advantages, including molecular sensitivity and intrinsic quantification. We anticipate that our methodology will have direct impact on a variety of fields including diagnostic biomarker detection and gene profiling.

Methods

SS-Nanopore Device Fabrication and Electrical Measurement

Nanopores were fabricated using a technique described elsewhere.[42] Briefly, the beam of a scanning helium ion microscope (Carl Zeiss Orion Plus) was focused on a suspended silicon nitride thin film membrane (thickness 30 nm) in a silicon support chip. Calibrated exposure times were used to mill nanopores with diameters ranging from 7.3 to 7.7 nm. The support chip containing an individual pore was then positioned in a custom flow cell with fluid access to both sides of the membrane. Measurement solution (900 mM NaCl and 6 mM PBS buffer) was introduced on either side of the flow cell, and Ag/AgCl electrodes were immersed in the solution. Electrical measurements (Axopatch 200B) were used to verify that the device exhibited low RMS noise (typically <20 pA) and linear current–voltage characteristics that matched the calibrated nanopore diameter.[32] Translocation measurements were performed by replacing the solution on one side of the device with measurement solution containing biomolecules. Current was recorded at a bandwidth of 200 kHz and filtered at 100 kHz with a four-pole Bessel filter. Analysis was performed with custom software with which we applied an additional low-pass filter of 25 kHz to all measurements. The event threshold for analysis was set at 4 standard deviations and events with durations from 12 to 2000 μs were considered.

Biomolecules

Bio90 oligonucleotides were purchased (Integrated DNA Technologies, Coralville, IA) with the sequence: TGT ATA CCA TGG CCA GGA TCC TGG GCC ATC TGG TAT^{B} GTA ATT CAT AAA GAA TTC TCA TTC TGC AGG TGC ACA TGT TAA CAC TAG TCG TGA. The T^{B} represents a single internal biotinylated dT. The opposing strand (forming the dsDNA) contained no modified nucleotides. The nonbiotinylated oligonucleotide used in the mixture (blind measurements) had the same sequence but with no biotin moiety. The streptavidin variant employed (SAe1D3) contained one active biotin-binding site[41] and was supplied by the Howarth lab (Oxford University). This mutant protein (54.5 kDa) retains binding affinity and stability similar to wild-type streptavidin and contains a hexaglutamate tag[43] used for isolation that imparts a negative charge of −17.1e under comparable pH conditions.

Electrophoretic Mobility Shift Assay

MS was incubated in 1× PBS buffer with bio90 for 20 min at room temperature at molar ratios ranging from 0:1 to 8:1 (MS:bio90). The mixtures were then loaded onto a 1.5% agarose gel with ethidium bromide for visualization. The buffer reservoir of the electrophoresis unit was submerged in an ice bath to minimize dissociation of the protein–DNA complex.

Supporting Information

Additional figures depicting recapture of translocated MS-DNA constructs, scatter plots as a function of applied voltage and stiochiometry, dwell time analysis, control measurements with nonbiotinylated DNA, and analysis of blind sample measurements. This material is available at the end of this formatted document.

Author Contributions

The manuscript was written through contributions of all authors. All authors have given approval to the final version of the manuscript.

A.T.C. and O.K.Z. contributed equally.

The authors declare no competing financial interest.

Acknowledgment

We thank the Howarth lab (Oxford University) for providing monovalent streptavidin and M. Marshall for helpful discussions. This work was supported by the North Carolina Biotechnology Center through Biotechnology Research Grant 2011-BRG-1201 and through start-up funds from Wake Forest University School of Medicine. J.R. and E.W.T. acknowledge funding from the Dr. Arthur and Bonnie Ennis Foundation, Decatur, IL.

References

1. Peng, J.; Schwartz, D.; Elias, J. E.; Thoreen, C. C.; Cheng, D.; Marsischky, G.; Roelofs, J.; Finley, D.; Gygi, S. P. Nat. Biotechnol. **2003**, 21 (8) 921– 926 Google Scholar

2. Rual, J.-F.; Venkatesan, K.; Hao, T.; Hirozane-Kishikawa, T.; Dricot, A.; Li, N.; Berriz, G. F.; Gibbons, F. D.; Dreze, M.; Ayivi-Guedehoussou, N.; Klitgord, N.; Simon, C.; Boxem, M.; Milstein, S.; Rosenberg, J.; Goldberg, D. S.; Zhang, L. V.; Wong, S. L.; Franklin, G.; Li, S.; Albala, J. S.; Lim, J.; Fraughton, C.; Llamosas, E.; Cevik, S.; Bex, C.; Lamesch, P.; Sikorski, R. S.; Vandenhaute, J.; Zoghbi, H. Y.; Smolyar, A.; Bosak, S.; Sequerra, R.; Doucette-Stamm, L.; Cusick, M. E.; Hill, D. E.; Roth, F. P.; Vidal, M. Nature **2005**, 437 (7062) 1173– 1178 Google Scholar
3. Zhang, B.; Park, B.-H.; Karpinets, T.; Samatova, N. F. Bioinformatics **2008**, 24 (7) 979– 986 Google Scholar
4. Jacinto, F. V.; Ballestar, E.; Esteller, M. BioTechniques **2008**, 44 (1) 35– 43 Google Scholar
5. Laird, P. W. Nat. Rev. Genet. **2010**, 11 (3) 191– 203 Google Scholar
6. Song, C.-X.; Yi, C.; He, C. Nat. Biotechnol. **2012**, 30 (11) 1107– 1116 Google Scholar
7. Williams, K.; Christensen, J.; Pedersen, M. T.; Johansen, J. V.; Cloos, P. A. C.; Rappsilber, J.; Helin, K. Nature **2011**, 473 (7347) 343– 348 Google Scholar
8. Hirai, M. Y.; Klein, M.; Fujikawa, Y.; Yano, M.; Goodenowe, D. B.; Yamazaki, Y.; Kanaya, S.; Nakamura, Y.; Kitayama, M.; Suzuki, H.; Sakurai, N.; Shibata, D.; Tokuhisa, J.; Reichelt, M.; Gershenzon, J.; Papenbrock, J.; Saito, K. J. Biol. Chem. **2005**, 280 (27) 25590– 25595 Google Scholar
9. Zhao, J.; Ohsumi, T. K.; Kung, J. T.; Ogawa, Y.; Grau, D. J.; Sarma, K.; Song, J. J.; Kingston, R. E.; Borowsky, M.; Lee, J. T. Mol. Cell **2010**, 40 (6) 939– 953 Google Scholar
10. Haring, M.; Offermann, S.; Danker, T.; Horst, I.; Peterhansel, C.; Stam, M. Plant Methods **2007**, 3, 11 Google Scholar
11. Selbach, M.; Mann, M. Nat. Methods **2006**, 3 (12) 981– 983 Google Scholar
12. Dekker, C. Nat. Nanotechnol. **2007**, 2 (4) 209– 215 Google Scholar
13. Wanunu, M. Phys. Life Rev. **2012**, 9 (2) 125– 158 Google Scholar
14. Freedman, K. J.; Haq, S. R.; Edel, J. B.; Jemth, P.; Kim, M. J. Sci. Rep. **2013**, 3, 1638 Google Scholar
15. Fologea, D.; Brandin, E.; Uplinger, J.; Branton, D.; Li, J. Electrophoresis **2007**, 28 (18) 3186– 3192 Google Scholar
16. Hoogerheide, D. P.; Garaj, S.; Golovchenko, J. A. Phys. Rev. Lett. **2009**, 102 (25) 256804 Google Scholar
17. Smeets, R. M. M.; Keyser, U. F.; Krapf, D.; Wu, M. Y.; Dekker, N. H.; Dekker, C. Nano Lett. **2006**, 6 (1) 89– 95 Google Scholar
18. Larkin, J.; Henley, R.; Bell, D. C.; Cohen-Karni, T.; Rosenstein, J. K.; Wanunu, M. ACS Nano **2013**, 7 (11) 10121– 10128 Google Scholar

19. Wanunu, M.; Sutin, J.; McNally, B.; Chow, A.; Meller, A. Biophys. J. **2008**, 95 (10) 4716– 4725 Google Scholar

20. Branton, D.; Deamer, D. W.; Marziali, A.; Bayley, H.; Benner, S. A.; Butler, T.; Di Ventra, M.; Garaj, S.; Hibbs, A.; Huang, X. H.; Jovanovich, S. B.; Krstic, P. S.; Lindsay, S.; Ling, X. S. S.; Mastrangelo, C. H.; Meller, A.; Oliver, J. S.; Pershin, Y. V.; Ramsey, J. M.; Riehn, R.; Soni, G. V.; Tabard-Cossa, V.; Wanunu, M.; Wiggin, M.; Schloss, J. A. Nat. Biotechnol. **2008**, 26 (10) 1146– 1153 Google Scholar

21. Niedzwiecki, D. J.; Iyer, R.; Borer, P. N.; Movileanu, L. ACS Nano **2013**, 7 (4) 3341– 3350 Google Scholar

22. Li, J.; Gershow, M.; Stein, D.; Brandin, E.; Golovchenko, J. A. Nat. Mater. **2003**, 2 (9) 611– 615 Google Scholar

23. Skinner, G. M.; van den Hout, M.; Broekmans, O.; Dekker, C.; Dekker, N. H. Nano Lett. **2009**, 9 (8) 2953– 2960 Google Scholar

24. Storm, A. J.; Chen, J. H.; Zandbergen, H. W.; Dekker, C. Phys. Rev. E: Stat., Nonlinear, Soft Matter Phys. **2005**, 71 (5 Pt 1) 051903 Google Scholar

25. Fologea, D.; Ledden, B.; McNabb, D. S.; Li, J. Appl. Phys. Lett. **2007**, 91 (5) 053901 Google Scholar

26. Plesa, C.; Kowalczyk, S. W.; Zinsmeester, R.; Grosberg, A. Y.; Rabin, Y.; Dekker, C. Nano Lett. **2013**, 13 (2) 658– 663 Google Scholar

27. Larkin, J.; Henley, R. Y.; Muthukumar, M.; Rosenstein, J. K.; Wanunu, M. Biophys. J. **2014**, 106 (3) 696– 704 Google Scholar

28. Bacri, L.; Oukhaled, A. G.; Schiedt, B.; Patriarche, G.; Bourhis, E.; Gierak, J.; Pelta, J.; Auvray, L. J. Phys. Chem. B **2011**, 115 (12) 2890– 2898 Google Scholar

29. Hall, A. R.; Keegstra, J. M.; Duch, M. C.; Hersam, M. C.; Dekker, C. Nano Lett. **2011**, 11 (6) 2446– 2450 Google Scholar

30. Prabhu, A. S.; Jubery, T. Z. N.; Freedman, K. J.; Mulero, R.; Dutta, P.; Kim, M. J. J. Phys.: Condens. Matter **2010**, 22 (45) 454107 Google Scholar

31. Venta, K.; Shemer, G.; Puster, M.; Rodríguez-Manzo, J. A.; Balan, A.; Rosenstein, J. K.; Shepard, K.; Drndić, M. ACS Nano **2013**, 7 (5) 4629– 4636 Google Scholar

32. Wanunu, M.; Dadosh, T.; Ray, V.; Jin, J.; McReynolds, L.; Drndić, M. Nat. Nanotechnol. **2010**, 5 (11) 807– 814 Google Scholar

33. Zhao, Q.; Sigalov, G.; Dimitrov, V.; Dorvel, B.; Mirsaidov, U.; Sligar, S.; Aksimentiev, A.; Timp, G. Nano Lett. **2007**, 7 (6) 1680– 1685 Google Scholar

34. Shim, J.; Humphreys, G. I.; Venkatesan, B. M.; Munz, J. M.; Zou, X.; Sathe, C.; Schulten, K.; Kosari, F.; Nardulli, A. M.; Vasmatzis, G.; Bashir, R. Sci. Rep. **2013**, 3, 1389 Google Scholar

35. Wanunu, M.; Cohen-Karni, D.; Johnson, R. R.; Fields, L.; Benner, J.; Peterman, N.; Zheng, Y.; Klein, M. L.; Drndic, M. J. Am. Chem. Soc. **2011**, 133 (3) 486– 492 Google Scholar

36. Gershow, M.; Golovchenko, J. A. Nat. Nanotechnol. **2007**, 2 (12) 775– 779 Google Scholar

37. Plesa, C.; Cornelissen, L.; Tuijtel, M. W.; Dekker, C. Nanotechnology **2013**, 24 (47) 475101 Google Scholar

38. Carlsen, A. T.; Zahid, O. K.; Ruzicka, J.; Taylor, E. W.; Hall, A. R. ACS Nano **2014**, DOI: 10.1021/nn501694n Google Scholar

39. Smoluchowski, M. v. Z. Phys. Chem. **1917**, 92, 129– 168 Google Scholar

40. Storm, A. J.; Storm, C.; Chen, J.; Zandbergen, H.; Joanny, J.-F.; Dekker, C. Nano Lett. **2005**, 5 (7) 1193– 1197 Google Scholar

41. Howarth, M.; Chinnapen, D. J. F.; Gerrow, K.; Dorrestein, P. C.; Grandy, M. R.; Kelleher, N. L.; El-Husseini, A.; Ting, A. Y. Nat. Methods **2006**, 3 (4) 267– 273 Google Scholar

42. Yang, J.; Ferranti, D. C.; Stern, L. A.; Sanford, C. A.; Huang, J.; Ren, Z.; Qin, L.-C.; Hall, A. R. Nanotechnology **2011**, 22 (28) 285310 Google Scholar

43. Fairhead, M.; Krndija, D.; Lowe, E. D.; Howarth, M. J. Mol. Biol. **2014**, 426 (1) 199– 214 Google Scholar

Supplementary Information

Selective detection and quantification of modified DNA with solid-state nanopores

Autumn Carlsen, Osama K. Zahid, Jan A. Ruzicka, Ethan W. Taylor, Adam R. Hall

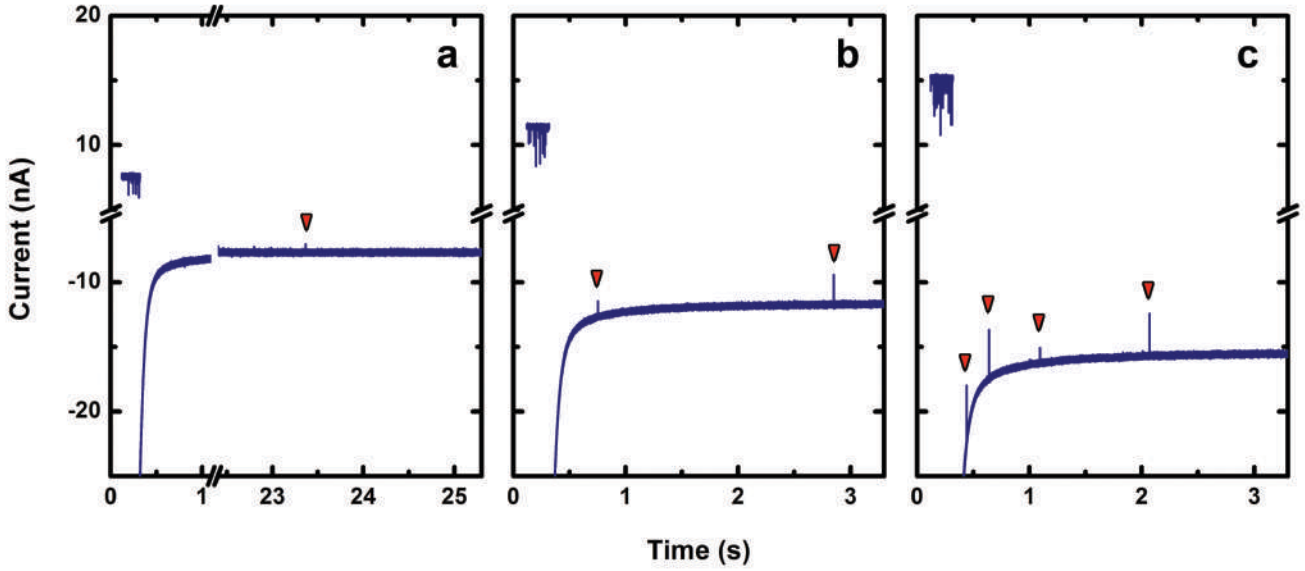

Supplementary Figure 1. Recapture of translocated MS-bio90 constructs. Raw current traces showing translocation events of MS-bio90 at positive bias (initial 0.25 s of each trace) followed by subsequent re-capture of translocated material at negative bias. Voltages applied are ±200 mV (a), ±300 mV (b), and ±400 mv (c). Red arrows indicate recapture events. As voltage is increased, we observe a higher efficiency of re-capture. These data demonstrate that the MS-bio90 events measured in our experiments correspond to constructs passing through the SS-nanopore.

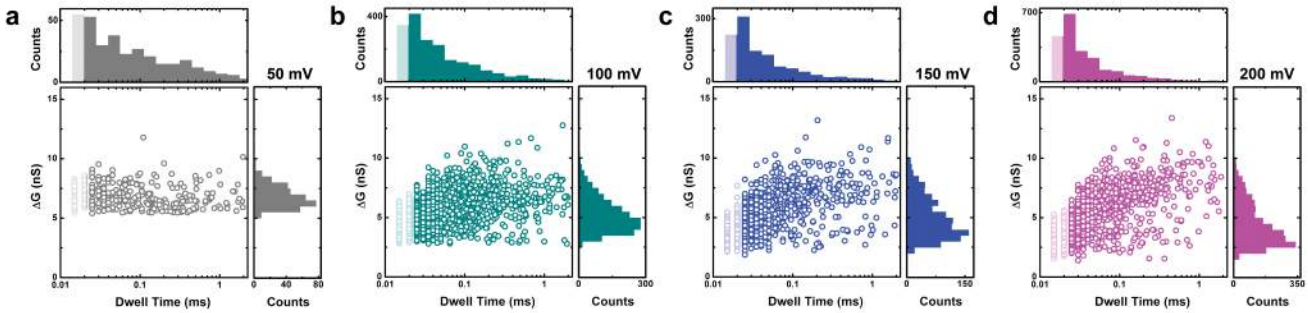

Supplementary Figure 2. Voltage dependence of scatter plots. Conductance blockage vs. dwell time for events measured at a stoichiometry of 1:1 (MS:bio90) and across a range of applied voltage (indicated at upper right of each plot). Total numbers of events considered are 332 (a), 1852 (b), 1129 (c), and 2193 (d). The faded population at the left of each plot represents events with duration below the resolution limit (25 μs). The ΔG histogram profile change may indicate multiple conformations of the MS-bio90 construct during translocation at higher voltage.

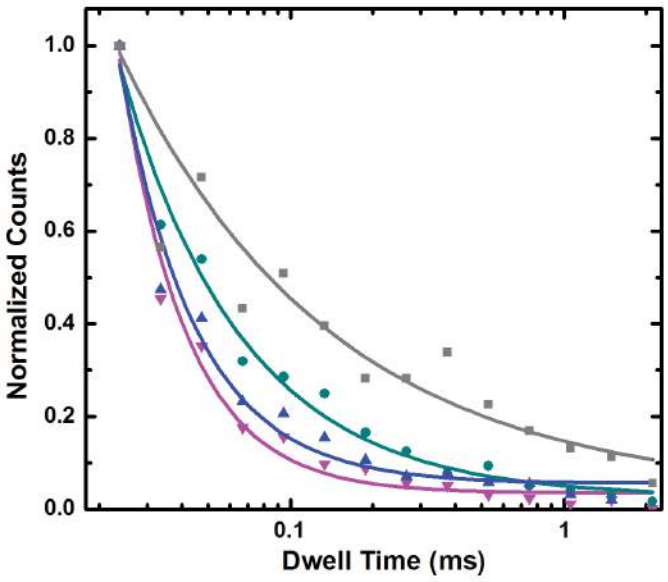

Supplementary Figure 3. Voltage dependence of MS-bio90 translocations. The normalized abundance of MS-bio90 dwell times, plotted from the resolution limit of 25 μs up to 2 ms (from the upper histograms in Supplementary Figure 2). Data displayed (T-B) are for applied voltages of 50 mV (grey squares), 100 mV (cyan circles), 150 mV (blue upward triangles), and 200 mV (magenta downward triangles), respectively. Solid lines are exponential fits to the (log-normal) data, demonstrating that event durations decay faster as applied voltage increase.

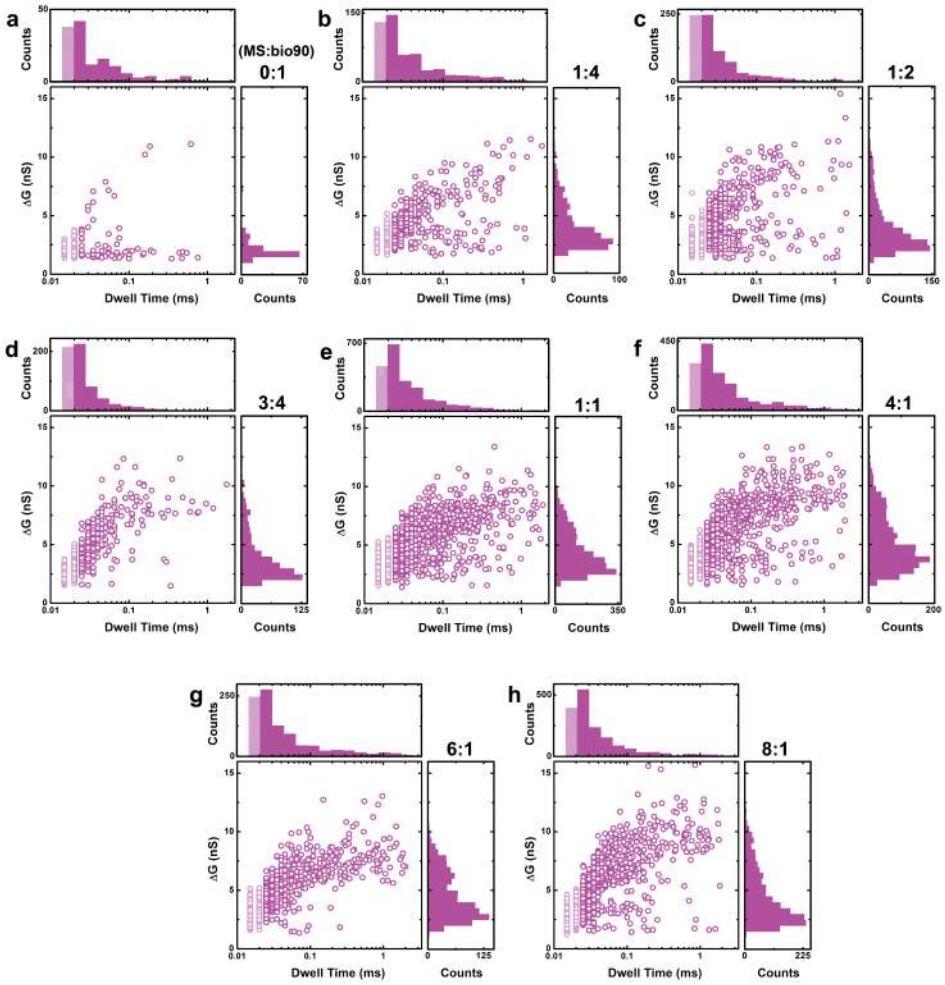

Supplementary Figure 4. Stoichiometry dependence of scatter plots. Conductance blockage vs. dwell time for events measured at an applied bias of 200 mV and across a range of stoichiometries (indicated at upper right of each plot). Total numbers of events considered are 139 (a), 521 (b), 816 (c), 642 (d), 2193 (e), 1528 (f), 982 (g), and 1652 (h). The faded population at the left of each plot represents events with duration below the resolution limit (25 μs).

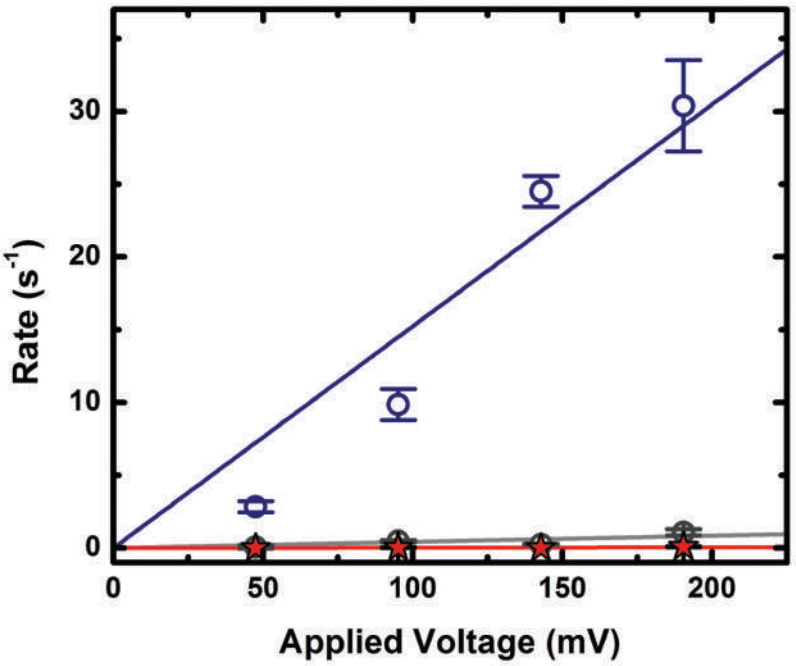

Supplementary Figure 5. Control measurements on non-biotinylated dsDNA. Measured event rate vs. applied voltage for MS mixed with non-biotinylated 95 bp dsDNA at a molar ratio (MS:DNA) of 4:1 (red stars). The mixture of MS and non-biotinylated DNA yields an extremely low event rate, more than an order of magnitude lower than bio90 mixed with MS at the same ratio (blue) and equivalent to that of bio90 with no added MS (grey). Solid lines are linear fits to the data.

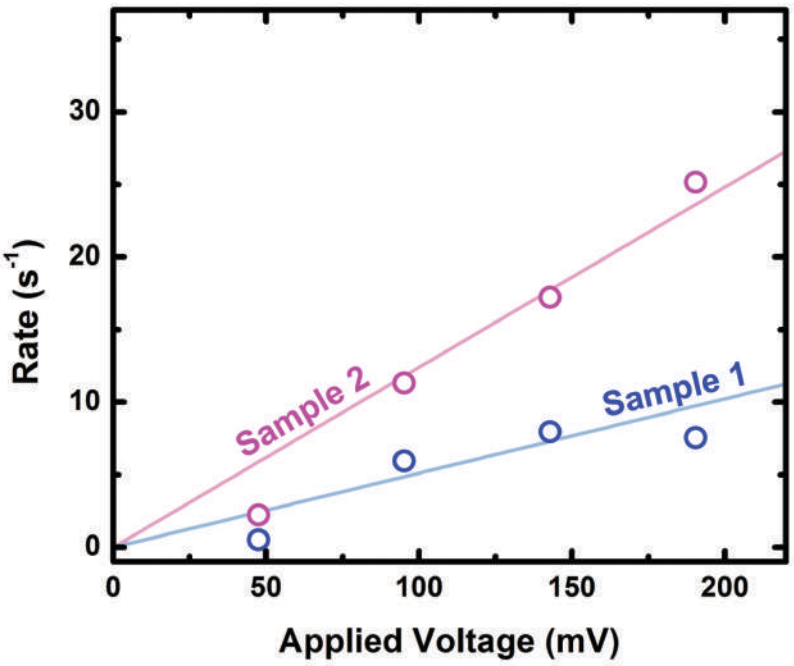

Supplementary Figure 6. Analysis of blind samples. Measured event rate vs. applied voltage for the two prepared admixtures (see Fig. 4). Solid lines are linear fits to the data (i.e. values plotted in Fig. 4).